Hail Damage to Typical Aircraft Surfaces

Robert J. Hayduk*
NASA Langley Research Center, Hampton, Va.

Severe structural damage can occur when aircraft collide with hailstones. Consequently, methods of predicting hail damage to airplane surfaces are needed by the aircraft designer. This paper describes an analytical method of predicting the dent depth and final deformed shape for simple structural components impacted by hailstones. The solution was accomplished by adapting the DEPROSS computer program to the problem of normal impact of hail on flat metallic sheets and spherical metallic caps. Experimental data and analytical predictions are presented for hail damage to typical aircraft surfaces along with a description of the hail gun and hail simulation technique used in the experimental study.

Introduction

THE collision of aircraft with hail can cause extensive damage to the aircraft, such as denting, tearing, and puncturing of the skin; shattering of the windshields; radome delamination; engine turbine blade pitting; and instrument damage. References 1–3 contain photographs exhibiting the variety of damage that can occur. Examples of typical structural damage are shown in Figs. 1. The leading edges and engine cowlings of this aircraft were extensively dented in a recent encounter with hail. Even though aircraft encounters with hail are infrequent, the severity of the structural damage which can occur is cause for concern and designers should be aware of the damage potential to aircraft surfaces. To provide the aircraft designer with a rational method of determining the damage potential of his aircraft before it actually encounters hail, analytical methods are needed for predicting the structural response of aircraft to hail impact.

An analytical method was devised at Langley Research Center for predicting denting-type hail damage to some typical aircraft surfaces. A hailstone impact simulator was developed to generate data to verify the analytically predicted damage. This paper describes the simulator and the analytical method; and then compares analytically predicted damage with some simulated hailstone damage data.

Hailstone Impact Simulation

Hailstone Impact Simulator

A schematic diagram and photograph of the hailstone impact simulator are shown in Figs. 2 and 3, respectively. The simulator consists of two major components: a launcher and a velocity measuring system. The launcher is composed of a barrel, coupling, reservoir, and two diaphragms. The coupling is sealed at each end by a frangible diaphragm to permit accurate control of the firing pressure. For example, to fire at a reservoir pressure of 12 MN/m^2, two diaphragms designed to rupture at 7 MN/m^2 are inserted in the coupling, a synthetic hailstone is placed in the chilled barrel, and the coupling bolted together. The coupling is pressurized first to 6 MN/m^2 and then the reservoir to 12 MN/m^2. Venting of the pressure in the coupling results in the rupturing of both diaphragms and the hailstone is subjected to the full 12 MN/m^2 reservoir pressure. Most of the hail data obtained with the simulator have been at velocities between 60 to 600 m/sec, which are typical of aircraft flight velocities. The hailstone impact simulator is capable of launching synthetic hailstones of any diameter by simply changing barrel size.

Velocity Measuring System

After the synthetic hailstone leaves the barrel, it enters the velocity measuring system which consists of two image converter tube cameras, two xenon-filled flashlamps, two fine tripwires, a scale, and an oscilloscope. The hailstone breaks the tripwire at each station and thus triggers the flashlamps. The cameras photograph the back-lighted hailstone and scale. The oscilloscope records the elapsed time between photographs and the scale establishes the hailstone's displacement during that time. The photographs of the hailstone in flight are also used to establish the integrity of the synthetic hailstone prior to impact.

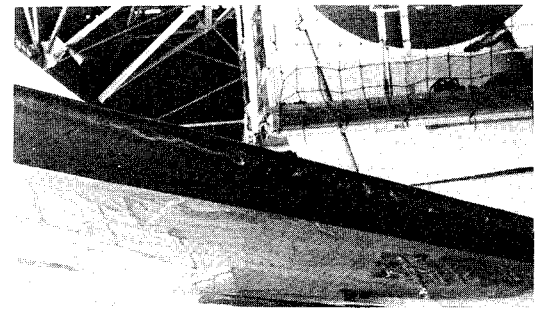

Fig. 1a Hail damage to horizontal stabilizer of a DC-8-61.

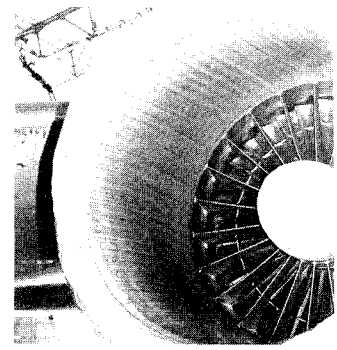

Fig. 1b Hail damage to engine cowling of a DC-8-61.

Presented as Paper 72-335 at the AIAA/ASME/SAE 13th Structures, Structural Dynamics, and Materials Conference, San Antonio, Texas, April 10–12, 1972; submitted May 9, 1972; revision received October 24, 1972.

Index categories: Aircraft Structural Design (Including Loads); Structural Dynamic Analysis.

*Aerospace Engineer, Strength Analysis Section, Structural Mechanics Branch, Structures Division.

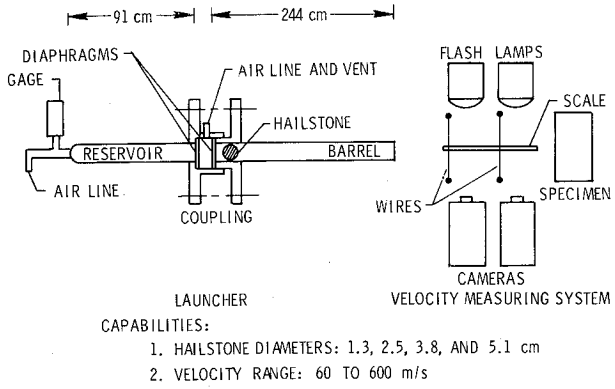

Fig. 2 Schematic diagram of hailstone simulator.

Synthetic Hailstones

Natural hailstones are usually formed in concentric layers as they move in convective storm clouds. They range in size from approximately 0.3 to 15 cm in diam. They usually have approximately conical shapes for sizes below 2 cm and roughly oblate spheroidal shapes for the larger sizes according to Ref. 4. Some researchers have suggested that the specific gravity of hailstones varies from 0.4 to 0.9 depending on the formation process.[1] Reference 4, however, states that "... the density of hailstones does not vary much ...."

With this information in mind, it was decided to produce synthetic hailstones by the simplest technique that would produce a conservative simulation of denting-type damage. Therefore, a technique was used to mold solid, spherical ice balls with a specific gravity of 0.93 from distilled water and alcohol. Figure 4 shows the lower half of a silicone rubber mold and four 5.1-cm-diam synthetic hailstones. To manufacture hailstones, the upper half of the mold is positioned and lightly clamped to the lower mold to prevent water leakage. The spherical cavities are filled with distilled water containing approximately 0.2% alcohol to prevent the formation of cracks during the freezing process. The molds are refrigerated at approximately 262°K (−11°C) to form synthetic hailstones. The solid synthetic hailstone should closely simulate the impact characteristics of natural hail, but will probably cause more structural damage than the natural hailstone.

In the present investigation hailstones from 1.3 to 5.1 cm in diam were used. This range of sizes represents the most frequently encountered hailstones as well as the sizes proposed in a design standard for supersonic transports.[5]

Test Specimens

Test specimens were modeled to reflect some of the typical shapes of aircraft surfaces. The specimens, shown in Fig. 5, represent a fuselage panel (flat sheet) and a nose or dome segment (spherical cap). All the specimens were made of 2024-T3 aluminum and were of two different thicknesses, 1.0 and 1.6 mm. The flat sheets are 35.6 cm square. The spherical caps have 20.3 and 40.6 cm radii of curvature and a sector angle of 45°.

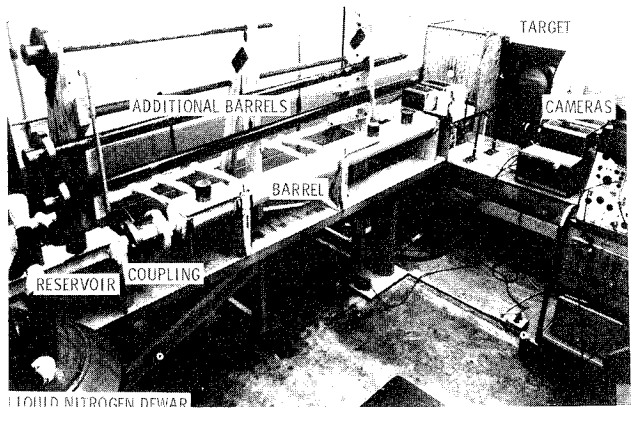

Fig. 3 Hailstone impact simulator.

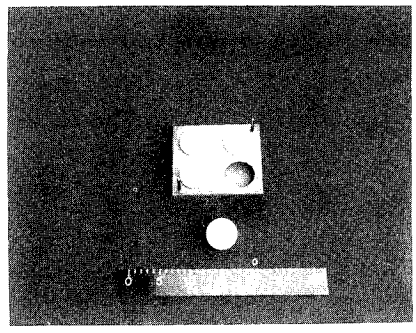

Fig. 4 Synthetic hailstones and mold.

Analytical Method

DEPROSS, a finite-difference computer program capable of analyzing the large deflection response of beams, rings, plates, and shells subjected to impulsive or blast loadings, was utilized to determine the dynamic, axisymmetric response of structures to hail impact. The material response can be elastic, elastic-plastic, elastic-strain hardening, or elastic-strain hardening-strain rate dependent. DEPROSS is described in detail in Refs. 6, 7, and 8. For this particular study, the initial velocity section of the computer program was modified to idealize the case of a hailstone impacting normal to the surface of a structure and crushing upon impact. The initial velocity distribution of the target with the added mass of the crushed hailstone was determined,[9] by assuming that the total momentum exchange upon impact was instantaneous and axisymmetric and that the hailstone does not rebound. The initial velocity distribution for the flat sheet is

$$w(\eta,0) = \frac{(K_1A/h)(\rho_p/\rho_s)g_0(1-\eta^2)^{1/2}}{1+(K_1A/h)(\rho_p/\rho_s)(1-\eta^2)^{1/2}};\quad 0 \le \eta \le 1$$
$$\dot{w}(\eta,0) = 0;\quad \eta \ge 1 \qquad (1)$$

where K_1 is a height factor defined below, A is the adjusted hailstone radius, h is the specimen thickness, ρ_p is the hailstone density, ρ_s is the specimen density, g_0 is the hailstone velocity, and $\eta = r/A$ is the nondimensional radial coordinate. For the spherical caps η is replaced by $(R/A)\sin\alpha$ and h is replaced by $h/\cos\alpha$, where $0 \le \alpha \le \sin^{-1}A/R$. R is the radius of curvature and α is the polar angle of the spherical caps.

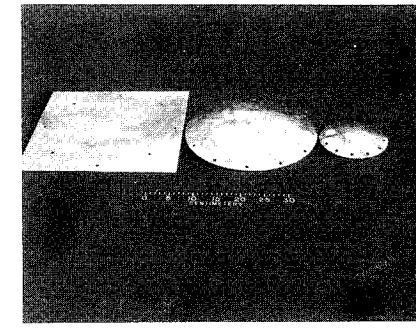

Fig. 5 Test specimens: flat sheet, 40.6 and 20.3-cm-radius spherical caps.

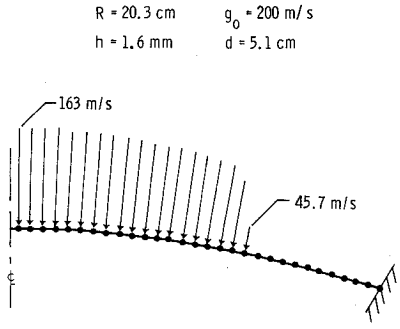

Fig. 6 Idealized computer model of a 5.1-cm-diam hailstone impact at 200 m/sec on a 20.3-cm radius, 1.6-mm-thick spherical cap.

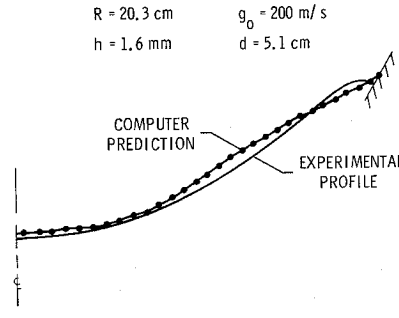

Fig. 7 Analytical and experimental profiles of a 20.3-cm radius, 1.6-mm-thick spherical cap after impact by a 5.1-cm-diam hailstone at 200 m/sec.

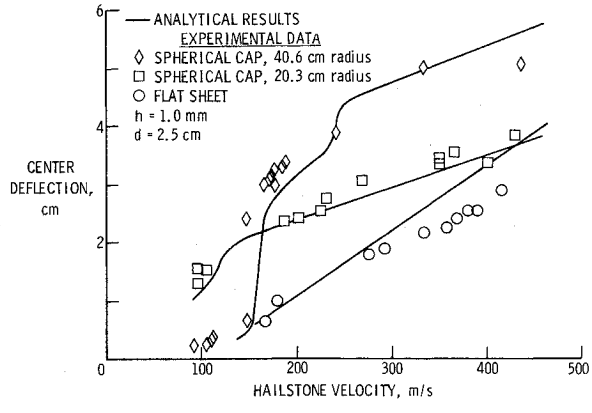

Fig. 8a Comparison of analytical and experimental center deflections of 1.0-mm-thick flat sheets and spherical caps impacted by 2.5-cm-diam synthetic hailstones.

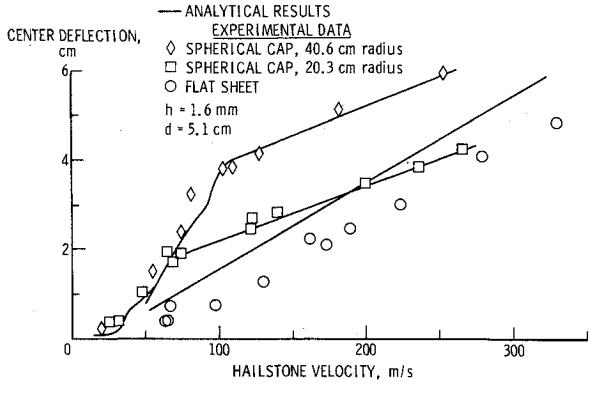

Fig. 8b Comparison of analytical and experimental center deflections of 1.6-mm-thick flat sheets and spherical caps impacted by 5.1-cm-diam synthetic hailstones.

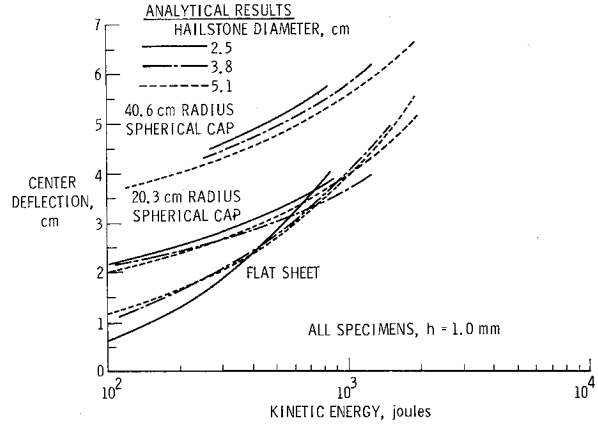

Fig. 9a Analytical results for 1.0-mm-thick flat sheets and spherical caps impacted by 2.5, 3.8, and 5.1-cm-diam synthetic hailstones.

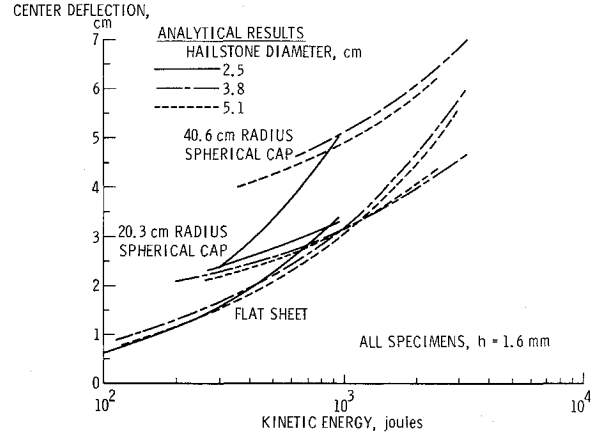

Fig. 9b Analytical results for 1.6-mm-thick flat sheets and spherical caps impacted by 2.5, 3.8, and 5.1-cm-diam synthetic hailstones.

The height of the hailstone was adjusted by the factor K_1

$$K_1 = 2/K_2^3 \tag{2}$$

to yield the same mass as the original uncrushed hailstone. The constant K_2 in this analysis represents the instantaneous spread of the radius of the hailstone (factor of 1.5 used) at impact.

The computer model of the structure consists of lumped masses (30 were used) connected by massless, extensible links as shown for the model of a 20.3-cm-radius spherical cap in Fig. 6. The sketch also shows the initial velocity distribution for the case of a 5.1-cm-diam hailstone impacting the shell at 200 m/sec. After the momentum exchange at impact, the velocity distribution ranges from 163 m/sec at the axis of symmetry to 45.7 m/sec at the outer mass station.

Results

The calculated final deformed shape and the experimentally determined cross section profile of the shell are shown in Fig. 7. At this velocity the entire shell has experienced an inversion of its original convex shape, termed snap-through, and the computer program adequately predicts the final deformed shape. However, at lower hailstone velocities, which do not initiate snap-through, there is only local denting of the shell. The computer program usually does not adequately predict this type of localized damage.

Figure 8 presents typical comparisons between analytical calculations and experimental data. In Fig. 8a the final center deflection or dent depth is plotted as a function of hailstone velocity for impacts of 2.5-cm-diam hailstones on flat sheets and spherical caps of 1.0 mm thickness. Similar information is presented in Fig. 8b for impacts of 5.1-cm-diam hailstones on specimens of 1.6 mm thickness.

For the spherical caps, the computer program closely predicts the velocity range over which snap-through occurs and the depth of the dent during and after snap-through. The theory predicts a linear response of center deflection with increasing velocity for the flat sheet and the spherical cap after snap-through. This behavior is substantiated by the data.

In Fig. 9 the analytical results are presented collectively on the basis of hailstone kinetic energy for three hailstone sizes and two specimen thicknesses. Figure 9a and 9b present the information for the 1.0- and 1.6-mm-thick specimens, respectively. In the figure, curves for spherical caps represent the specimen's center deflection after snap-through. For example, in Fig. 8b snap-through of the 40.6-cm-radius spherical cap is complete at 107 m/sec. The linear portion of the curve for velocities between 107 and 274 m/sec is represented in Fig. 9b by the dashed (-----) curve for the 40.6-cm-radius spherical cap.

With the exception of the analytical curve in Fig. 9b for 2.5-cm-diam hailstone impacts on 40.6-cm-radius spherical caps, the analytical curves for the three specimens band together. The analytical curves for the spherical caps reasonably represent the actual center deflections as demonstrated in Fig. 8. However, the analytical results for the flat sheets are generally conservative. For a particular hailstone kinetic energy, the figures can be used to make a reasonable estimate of the center deflection that would occur in these specimens.

The anomalous behavior of the 2.5-cm-diam hailstone results in Fig. 9b can possibly be explained by examining Fig. 8a. The analytical curve for the 40.6-cm-radius spherical cap indicates that the snap-through region does not necessarily have to be a smooth transition. In this case, a region of very steep slope is followed by a second region of smaller slope. However, this second region still has a much larger slope than the portion of the curve beyond snap-through, that is, for velocities greater than 250 m/sec. The anomalous curve in Fig. 9b could be an extensive, linear second snap-through region rather than the linear region after snap-through.

Concluding Remarks

The hailstone impact simulator is a valuable laboratory apparatus which can be used for such hailstone research as the testing of prospective structural designs or generating data to compare with theory. It has been successfully used to obtain deformation data on flat sheets and spherical caps of various sizes impacted by synthetic hailstones at typical aircraft flight velocities.

The computer program described here adequately predicts the damage to a simple structure when impacted by a hailstone. However, the program is restricted to axisymmetric structures impacted normally at the axis of symmetry.

References

[1]Souter, R. K. and Emerson, J. B., "Summary of Available Hail Literature and the Effect of Hail on Aircraft in Flight," TN 2734, 1952, NACA.

[2]Roys, G. P., "Airborne Instrumentation System for Measuring Meteorological Phenomena Inside Thunderstorms," ASD-TDR-63-231, May 1963, Wright-Patterson Air Force Base, Ohio.

[3]Williamson, R. E., "Aircraft Probing of Hailstorms," MR169 FR-841, Jan. 1969, Inst. of Atmospheric Sciences, South Dakota School of Mines and Tech., Rapid City, S. D.

[4]Knight, C. and Knight, N., "Hailstones," *Scientific American*, Vol. 224, No. 4, April 1971, pp. 96–103.

[5]"Hail Criteria for Airworthiness Purposes," Working Paper 8.2.2.06 presented at the *FAUSST VIII Meeting*, Jan. 25–29, 1971, Federal Aviation Administration, Washington, D.C.

[6]Leech, J. W., Pian, T. H. H., Witmer, E. A., and Herrmann, W., "Dynamic Response of Shells to Externally-Applied Dynamic Loads," ASD-TDR-62-610, Nov. 1962, Wright-Patterson Air Force Base, Ohio.

[7]Witmer, E. A., Balmer, H. A., and Pian, T. H. H., "Large Dynamic Deformations of Beams, Rings, Plates, and Shells," *AIAA Journal*, Vol. 1, No. 8, Aug. 1963, pp. 1848–1854.

[8]Balmer, H. A., "Computer Programs to Calculate the Dynamic Elastic-Plastic Axisymmetric Responses of Impulsively Loaded Circular Plates and Shells of Revolution," ASRL TR 128-2, Dec. 1964, MIT, Cambridge, Mass.

[9]Thomson, R. G., Hayduk, R. J., and Alfaro-Bou, E., "The Denting of Aircraft Surfaces by Hail," presented at the *FAUSST VIII Meeting*, Washington, D.C., Jan. 25–29, 1971.